Radar Design for Determining the Strength of Tropical Cyclones in the Bay of Bengal

by Harold W. Baynton*

A Technical Report (1977)

Prepared by:
Monitoring and Assessment Research Centre of the
Scientific Committee on Problems of the Environment,
International Council of Scientific Unions

With the support of
United Nations Environment Programme and
The Rockefeller Foundation

* Present address: National Center for Atmospheric Research, Boulder, Colorado, U.S.A

PREFACE

Unlike those environmental problems which are generated by human activities, naturally induced problems, *i.e.* natural disasters such as earthquakes, land-slips, great winds, giant waves, floods and droughts, virtually defy control. This places a premium on prediction and other early warning techniques for their avoidance which stretch current scientific understanding and technological skills to their limits.

Year after year the toll of deaths and human suffering is a grim reminder of the fact that our success rate is low. This is why the UN Environment Programme has made natural disasters one of its priorities and stressed that "greater attention should be given to disaster preparedness and prevention, including mitigation and early warning".

An especially severe and recurring natural disaster is the tropical cyclone particularly as affecting the land surrounding the Bay of Bengal and the Arabian Sea. A particularly well documented case there was the cyclone of 1970, when an estimated 300,000 people died. Although it is possible to predict the occurrence of a cyclone from satellite pictures, it is almost impossible to make a precise estimate of its severity. The decision whether or not to warn the public of approaching danger is thus a very difficult one to make. Repeated death and destruction can best be minimized if killer storms can be distinguished from non-killer storms and thus assure public acceptance of warning systems. Aircraft reconnaissance into the storm centres is one way, but the cost of maintaining an aircraft alert system is prohibitively high. Modern Doppler radar equipped with a real-time processor and colour display appears to offer a less costly alternative. The ensuing report develops a specification for such a cyclone detecting radar from a new radar technology proven in use at the National Center for Atmospheric Research, Boulder, Colorado, USA.

Recently, the World Meteorological Organization and the UN Environment Programme initiated a project to prepare schemes for Bangladesh, Burma, India, Pakistan, Sri Lanka and Thailand to improve their existing cyclone monitoring and warning systems. It is hoped that the present report will make a timely and useful contribution to this very important project.

Gordon T. Goodman,
Director

Radar Design for Determining the Strength of Tropical Cyclones in the Bay of Bengal

1.0 Introduction

One of the goals of the United Nations Environment Programme (UNEP) is that there should be warnings of natural disasters. Among these disasters is the tropical cyclone, known also as the hurricane and typhoon. Of the half dozen regions that experience these storms, Bangladesh historically has been the most severely affected. There the problem is aggravated by the large tidal range, up to 5 m, over the northern tip of the Bay of Bengal. If the storm surge induced by cyclonic winds is in phase with high tide, the resulting floods may be disastrous.

A recent example brings the problem into focus. On 12 November 1970 a tropical cyclone with maximum winds of about 100 knots (kt) crossed the coast of Bangladesh. Frank and Husain (1971) described this storm as "the deadliest tropical cyclone in history". Due primarily to the accompanying storm surge — up to 4 m in places — 300,000 people perished. The track of the storm can be seen on Figure 1.

Each year about 12 tropical depressions develop over the Bay of Bengal (Frank and Husain, op. cit.). On the average, five of these become cyclonic storms with winds of 40 kt or more and an occasional one intensifies into a killer storm. Since tropical cyclones are often no more than 500 km in diameter, they may easily exist over the vast Bay of Bengal with no telltale evidence along the coast.

The cyclone warning centres around the Bay of Bengal depend heavily on satellite photos. Satellites are indispensable for providing early warning of tropical depressions and there has been progress in classifying cyclone intensity from satellite images (Dvorak 1972). Koteswaram (1971) reported that US criteria for predicting hurricane intensity from satellite pictures appeared to offer useful guidance when applied to Indian Ocean cyclones. Sikka (1971) compared storm intensity in the bulletins issued by the Storm Warning Centres at Calcutta and Bombay with the intensity based on satellite pictures. The following categories of intensity were used.

Depression	—	winds 17–27 kt
Deep depression	—	winds 28–33 kt
Tropical storm	—	winds 34–47 kt
Severe tropical storm	—	winds 48 kt and above.

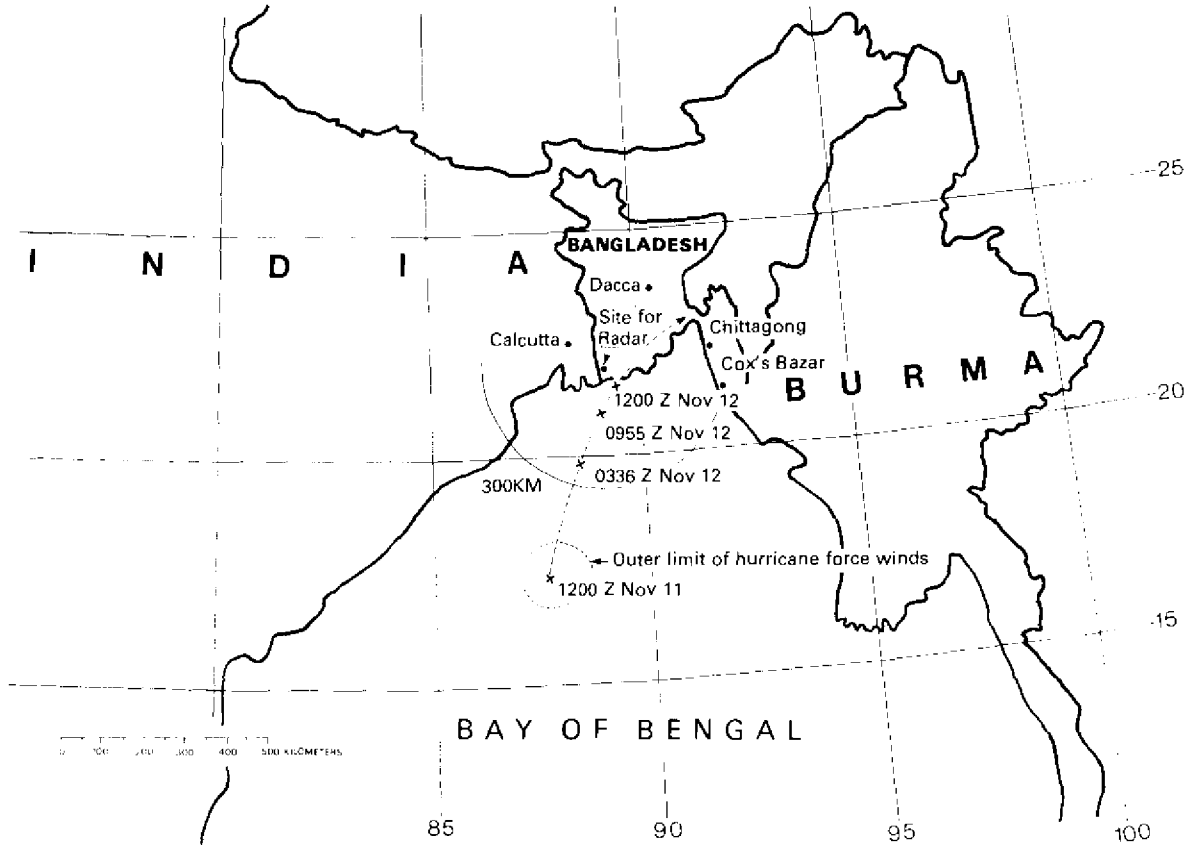

Figure 1. Map of the Bay of Bengal showing track of the tropical cyclone that devastated Bangladesh on 12 November 1970. Possible site for radar is at 21.9 N., 89.1 E.

Sikka's analysis included 155 comparisons with the Washington global readout picture and 182 with the APT* picture received at Bombay. Table 1, below, based on Sikka's extensive tables, allows us to consider the number of cases when the storm bulletin and the satellite inference agreed exactly and when they disagreed by one category as to storm intensity.

Table 1 Comparison of storm intensity in the operational storm bulletin and the intensity inferred from satellite pictures.

	Exact agreement per cent	Disagreement by one category per cent	Disagreement by more than one category per cent
Washington picture	45	35	20
APT picture	49	35	16

Sikka recommended that, in the absence of ship reports near the centre of a storm, the satellite inference should be used. However, from the standpoint of disaster warnings, the real need is to be able to make finer distinctions within the category "severe tropical storm". Satellite images alone are simply incapable of doing this.

The satellite capability is supplemented by a few non-Doppler radars situated along the coast of the Bay of Bengal, for example at Cox's Bazar. Although these radars can track the movement of the tropical cyclones, they provide no direct measurement of wind speeds. Lacking precise information on storm intensity, the storm warning centres have shown an understandable bias towards over-warning. Public apathy has resulted. In their report on the Bangladesh cyclone disaster of 1970, Frank and Husain noted that over 90 per cent of the people in the disaster area knew about the storm yet less than one per cent sought refuge in more substantial buildings.

Clearly the problem is to distinguish between killer and non-killer storms. Writing in 1971, Frank and Husain could assert that aircraft reconnaissance provided the only practical way of determining the strength of a cyclone before it reached the coast. It is proposed here that, with recent advances in data processing, modern, shore-based Doppler radar provides a viable alternative to aircraft reconnaissance. The procedure will be to develop the performance specifications for a

* Automatic picture transmission

cyclone detection radar and then to test its diagnostic ability against a reconstruction of the wind field of the 1970 storm.

2.0 Radar System Specifications

We need not be concerned with complete hardware specifications but only with those characteristics bearing on the diagnosis of tropical cyclones. We shall need a radar that is capable of measuring wind speed and rainfall rate. All radars measure reflectivity, which can be used to estimate rainfall rate. A Doppler radar, in addition, measures the radial velocity component of the targets that it detects. The measurement is based on the shift in frequency that moving targets produce between the transmitted and backscattered signals. It has been shown that the radial velocity of the target, V_R, is related to this Doppler shift, f, and the wavelength, λ, of the transmitted signal by the expression

$$V_R = f\lambda/2.$$

In order to measure the Doppler shift, either the frequency of the backscattered signal must be compared with the frequency of the transmitted signal, or both frequencies must be compared to a common reference. If each transmitted signal pulse consists of a segment of an unbroken pure sine wave, the frequency of the backscattered signal may be compared directly to the frequency of the transmitted signal. Radars that operate in this way are called *coherent* Doppler radars and are preferred, for meteorological use, over non-coherent Doppler radars that employ an external reference frequency. We therefore specify a coherent Doppler radar.

Modern coherent Doppler radars use a slight variant of the procedure whereby the phase change between consecutive backscattered pulses becomes the measure of radial velocity. In meteorological applications, collections of falling precipitation particles provide the targets. As the particles fall they are swept along by the wind and, except in the case of large hailstones, it is safe to assume that their horizontal velocity is a good approximation to the horizontal wind speed.

Because of the considerable range at which we will wish to view the cyclones and the very intense horizontal gradients of wind speed near cyclone centres, we specify a relatively narrow one-degree pencil beam. At ranges of 200 and 300 km this will give beam widths of 3.49 and 5.24 km.

There is a case for preferring a half-degree beam, especially at ranges of 200-300 km, because of the better spatial resolution and improved beam filling (hence greater sensitivity) that would result. However, since antenna diameter is inversely proportional to beam width, the choice of half degree would double the size of the antenna, its pedestal and the protective radome, at a very substantial increase in costs. Gray and Shea (1976), in their summary of 533 radial penetrations of hurricanes, found it advantageous to average wind speeds over 2.5 nautical mile (4.63 km) flight segments, in order to eliminate small scale fluctuations in the data. Evidently a one-degree beam can provide adequate spatial resolution. On economic grounds, therefore, a one-degree beam is specified. The performance penalty will be instances of weak signal at great range, a limitation unlikely to affect the detectability of the more severe tropical cyclones.

We must also specify the radar wave length, λ , the pulse repetition frequency (PRF) and the capability of the associated data processing and display system. Eventually we will also want to specify transmitter power, pulse duration and receiver sensitivity but it is convenient to defer this until Section 7 where errors and limitations of the procedures are discussed.

2.1 Preliminary Design Considerations

A pulsed Doppler radar transmits a short pulse — a few microseconds — of microwave energy in a narrow beam. It then waits a relatively long time — a few thousand microseconds — to receive energy reflected from targets before sending the next pulse. The range of a target is determined from the time taken for the pulse to go out to the target and back. If the reflected energy from a distant target arrives back after the next pulse has been transmitted, it may be confused with energy from the next pulse reflected by a close in target. There is, therefore, a maximum unambiguous range, R_{max}, for every pulsed radar, given by

$$R_{max} = \frac{C}{2(PRF)} \qquad (1)$$

where C is the velocity of light, 3×10^5 km/sec, and PRF is the pulse repetition frequency of the radar, typically in the range 200 to 1200 per second. In practice the useful range of the radar is its maximum unambiguous range, which can be extended by decreasing the PRF. If the PRF is 1000 pulses per second, the maximum unambiguous range

is only 150 km whereas it increases to 500 km if the PRF is reduced to 300 pulses per second.

The speed of a target, towards or away from the radar, is computed by comparing the phases of the microwaves in consecutive reflected pulses. Targets that are either stationary or moving tangentially to the radar beam will produce no phase change. If the phase change is positive and exactly equal to one-half wave length, it is indistinguishable from a negative phase change of exactly one-half wave length. There is, therefore, also a maximum unambiguous velocity, V_{max}, given by

$$V_{max} = \pm (PRF)\, \lambda /4. \qquad (2)$$

In meteorological practice it is difficult, but not impossible, to resolve velocities greater than the maximum unambiguous velocity. It is therefore desirable to make V_{max} as large as possible. We do this by choosing a large λ since we have noted earlier that we wish to keep the PRF small in order to extend the unambiguous range. However, before specifying the pulse repetition frequency and the wavelength, we must consider the effects of earth curvature and refraction on radar performance.

2.2 Earth Curvature and Refractive Effects

The practice of watching for distant targets with radar is constrained by earth curvature. The downward bending of microwaves by a standard atmosphere compensates slightly for earth curvature. For average refraction the net effect is represented, approximately, by imagining that a ray travels in a straight line, and the earth's radius is four-thirds times its actual radius (Freehafer 1951). This four-thirds-earth-radius treatment of earth curvature and refraction leads to the following equation for ray tracing.

$$Z = \frac{R^2}{17{,}000} + R \sin \alpha + Z_0 \qquad (3)$$

Here Z is the height above mean sea level of the ray in kilometres, at a slant range of R kilometres, α is the elevation angle of the ray, and Z_0 is the height of the radar above sea level in kilometres. The development of equation (3) appears in Appendix 1.

When a radar looks across the sea, there is some elevation angle for

which the ray is tangent to the sea. For a radar at sea level, this elevation angle is 0 degrees and the point of tangency is at the radar. As the radar is raised in elevation, on a hill or mountain, the tangential elevation angle becomes less than zero and the point of tangency will be at some distance from the radar. Equation (3) can be used to compute the tangential elevation angle and the slant range to the point of tangency for selected values of radar height. The results of such computations are presented graphically in Figure 2.

Figure 2 suggests that one may extend the range by locating the radar on a hill. However, unless the hill is at the coastline, any gains from elevating the radar tend to be lost by distance back from the coastline. In the case of Bangladesh, the radar will be effectively at sea level although it may need to be several kilometres inland to reduce the threat of flooding.

At a range of 300 km a tangential radar beam will reach a height of 5.29 km. Since at that range a one-degree beam will be 5.24 km wide, the beam will fill the region 5.29 ± 2.62 km. Similarly, at a range of 500 km the beam will have risen to 14.71 km, filling the region 14.71 ± 4.36 km. Studies of Atlantic hurricanes and Pacific typhoons by Jordan (1952) and of Atlantic hurricanes by Shea and Gray (1973) showed that wind speeds were still nearly as strong at heights of 5 to 6 km as in the boundary layer, but had undergone quite substantial change by 10 km. Colón *et al.* (1970) confirmed the essential similarity of Indian Ocean cyclones to those in other regions of the globe. Clearly it is useful to examine the wind structure of cyclones at a height of up to 5–6 km, *i.e.*, at a slant range of up to 300 km, but pointless to carry it beyond 300 km. We therefore propose a pulse repetition frequency of 500 per second and a wavelength of 0.107 m. Substituting these values in equations (1) and (2) we get a maximum unambiguous range of 300 km and a maximum unambiguous velocity of ± 13.38 m/sec (26.0 kt). Section 2.4, below, describes how velocities greater than the maximum unambiguous velocity can be measured by means of an ingenious coloured display.

It should be noted that the choice of wavelengths is limited to one of the three bands, X, C, or S, in use in meteorological radars. A set of letter band-designations was introduced as a wartime security measure to conceal the frequencies being used. Although each band specifies an interval of wavelengths, in meteorological practice X-, C- and S-band are commonly taken to mean wavelengths of 3.2, 5.6 and 10.7 cm, respectively. We have selected the S-band.

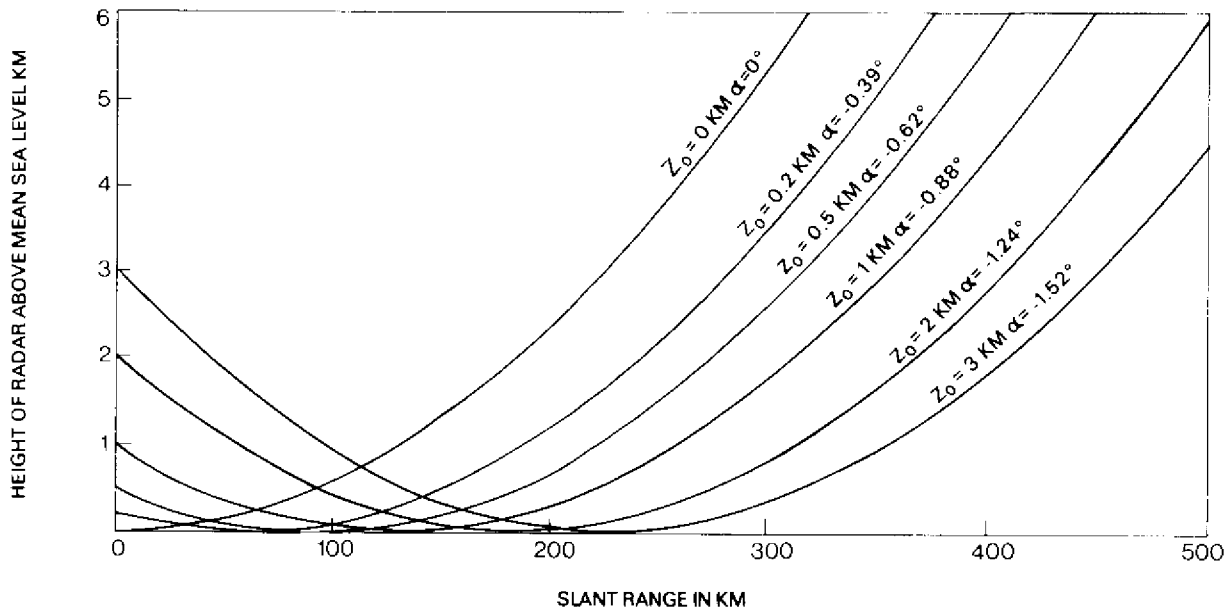

Figure 2. Path of rays tangential to the earth with average refraction for various radar heights, Z_0. Tangential elevation angles, α, are shown on the ray paths.

With the specification of wavelength, λ, the size of the antenna can also be established. A pencil beam is produced by a circular paraboloid antenna whose diameter, d, is given, approximately, by the expression

$$d = \left(\frac{5}{4}\right) \left(\frac{57.3}{E}\right) \lambda$$

where E is the beam width in degrees. Thus a one-degree beam and a wavelength of 0.107 m requires an antenna diameter of approximately 7.7 m.

2.3 Microwave Attenuation

Microwave attenuation increases with rainfall rate. At X-band it represents a serious constraint; at C-band it is often tolerable, especially in the tropics, while at S-band it is insignificant. Senn (1971) confirmed this for tropical cyclones. He observed three hurricanes over a 72 n.mi. path at a rainfall rate of about 1 in./hr and obtained attentuations of 87, 29 and $\leq$ 4 dB at X-, C- and S-band, respectively. Low attenuation is mandatory since we wish to examine the cyclone structure at long range and will often have to propagate the radar waves through intense intervening rainfall. The lack of attentuation at S-band also permits more reliable estimates of rainfall rate, at least at close range when the beam is close to the ground. These will contribute to better estimation of the stream flooding to be expected after the cyclone has moved inland.

2.4 Data Processing

The radar will be equipped with a digital radar processor and a minicomputer to perform the following operations.

(1) To process the Doppler information in real time into a record of radial velocities (Lhermitte 1972).
(2) To control the display of the velocities on a coloured television monitor in a standard PPI (plan-position indicator) format.
(3) To control the recording of the velocity and reflectivity factor on magnetic tape.

Radars equipped in this way have been developed at the National Center for Atmospheric Research (NCAR), Boulder, Colorado, USA. Details of their construction and operation are given by Gray *et al.* (1975). They have been used successfully in extratropical cyclonic

storms of temperate latitudes (Baynton *et al.* 1977). Winds of 70 m/sec (136 kt) have been observed although the maximum unambiguous velocity was only 14.6 m/sec. In 1976 the writer participated in a field programme of the National Hail Research Experiment, near Grover, Colorado, when the complex airflow of a hail supercell (Browning and Foote 1976) was graphically displayed in colour. There is every reason to believe that similar radars can be applied successfully to tropical cyclones which lie between hail storms and extratropical cyclones in size.

The NCAR system uses 15 colours, thus requiring more than one shade of red, yellow, blue, green, etc. Experience has shown that it is difficult to distinguish betweeen shades of the same colour, especially when there are strong gradients of wind speed. Since very large gradients are encountered in tropical cyclones, it is proposed that only seven colours should be used for this application.

Figure 3 shows how the seven colours, purple, blue, green, grey, brown, yellow and red may be used to encode the velocity within the unambiguous range, −26.0 to +26.0 kt. The width of each colour band is 7.42 kt given by 2(26.0) ÷ 7. The television monitor can be thought of as a fine mesh grid. Each square of the grid is assigned one of the seven colours corresponding to the observed radial velocity of targets, or black if there are no targets. Grey is used to indicate targets with radial velocities of 0 ± 3.7 kt. It is referred to as the "zero velocity" band. Ground clutter, as well as all targets viewed from the side, no matter how fast they are moving, have zero radial velocity and therefore appear grey.

Figure 3 also illustrates how velocities outside the unambiguous range will be encoded. It is analogous to a basic scale of musical notes with which there are associated octaves both above and below the basic scale. Outside the unambiguous velocity range the colours repeat themselves in the same order in which they appear within the unambiguous range. Although there is thus not a one-to-one correspondence between a colour and a velocity interval, the potential ambiguities are readily resolved within the context of the full colour pattern. This will become apparent later when examples of tropical cyclone echoes are presented in colour.

An essential feature of the colour display system is a zoom control that permits the operator to magnify a portion of the field two, four, or eight times. Figure 4 illustrates the four optional presentations. Figure 4 (a) is the basic PPI display of the total radar field out to the full

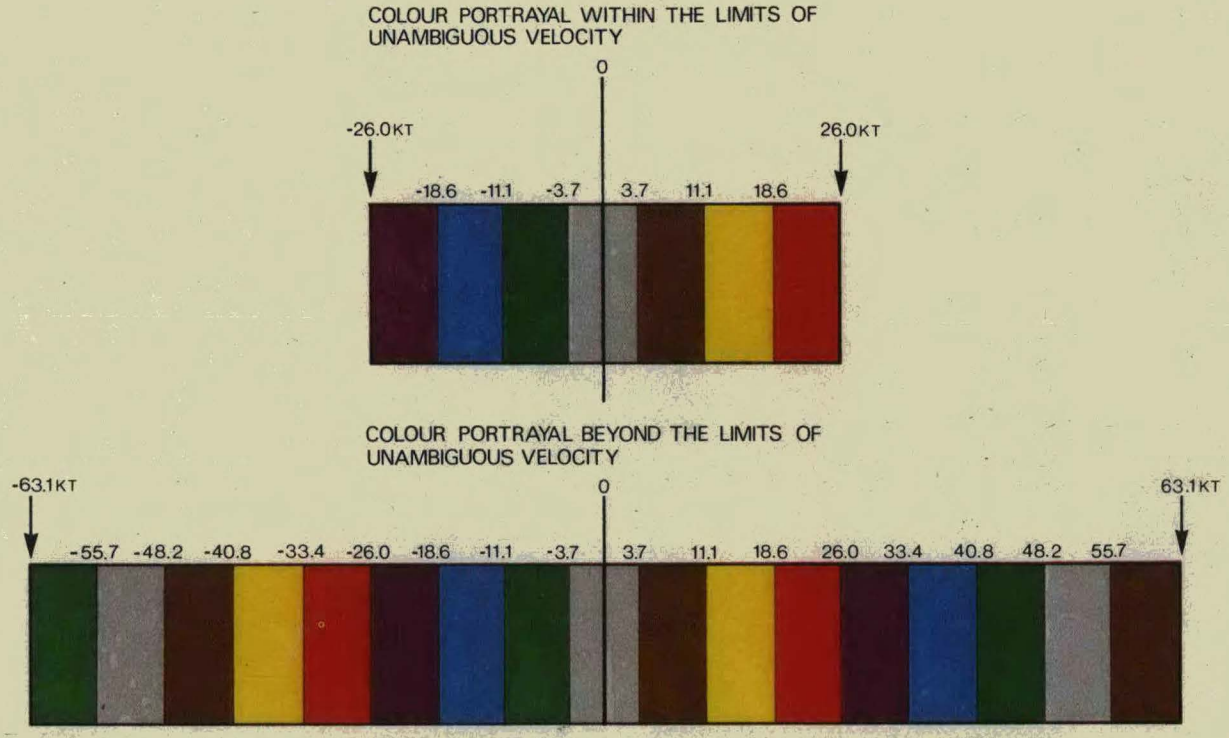

Figure 3. Velocity encoding in seven colours within the unambiguous velocity interval (upper) and beyond the unambiguous velocity interval (lower).

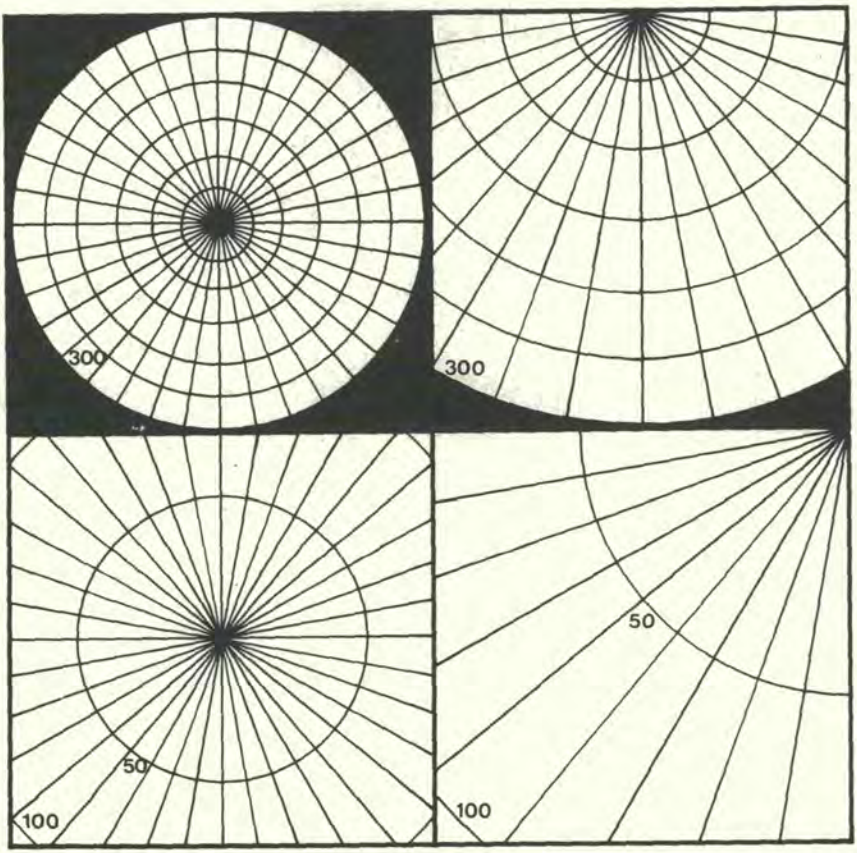

Figure 4. Formats of coloured PPI radar presentation at various magnifications. For magnifications of 2, 4 and 8, segments other than those shown can be selected. All range marks are at 50-km intervals, bearings are at 10-degree intervals.

unambiguous range of 300 km. This is the normal mode during preliminary surveillance. A control on the data console allows the operator to select the portion of the total field that will be magnified. Twofold magnification, (b), would probably be practical for monitoring tropical cyclones. Fourfold magnification, (c), has been used when scanning extratropical cyclones at higher elevation angles and the eightfold magnification, (d), has been limited to studies of thunderstorms.

3.0 Structure of the 1970 Bangladesh Cyclone

For the present analysis we postulate a radar located at 21.9 N. 89.1 E. as shown on Figure 1. In 1971 a radar was being proposed for Khepupara at about this location but it seems not to have been installed. The point 21.9 N. 89.1 E. will be referred to as "the radar site" although no radar existed there in 1970.

Frank and Husain (op. cit.) provide the most complete data on the structure of this storm. Its track, based on satellite photographs by ITOS 1, is shown in Figure 1. Winds may have reached 100 kt by the time it moved inland 80 km north-west of Chittagong. An anemometer at Chittagong blew down just after registering 78 kt. At 0600Z on 12 November the cyclone centre is estimated to have been 200 km from the radar site on a bearing of 196 degrees and to have been moving on a heading of 23 degrees at a speed of about 15 kt. The cyclone vortex had a diameter of six to seven degrees of latitude as viewed from the satellite.

For a detailed reconstruction of the kind of wind field that probably existed, we must resort to reports of the average structure of Atlantic hurricanes (Shea and Gray op. cit.) and of Pacific typhoons (Hughes 1952), in both cases based on aircraft reconnaissance. Shea and Gray summarized the average structure of a hurricane based on 533 radial legs flown on 41 days into the centre of 21 hurricanes between 1957 and 1969. They avoided much of the smoothing inherent in averaging by measuring distances from the observed radius of maximum wind speed. After the manner adopted by Hughes, they normalized their data with respect to the storm heading and summarized tangential and radial components as shown in Figure 5. Hughes had summarized 84 flights into 28 Pacific typhoons. Whereas the Shea and Gray data are very detailed near the eye of the hurricane, but extend only out to 50 nautical miles (n.mi.) the Hughes data, shown in Figure 6 are simply estimates within 30 n.mi. of the eye but extend out to 300 n.mi.

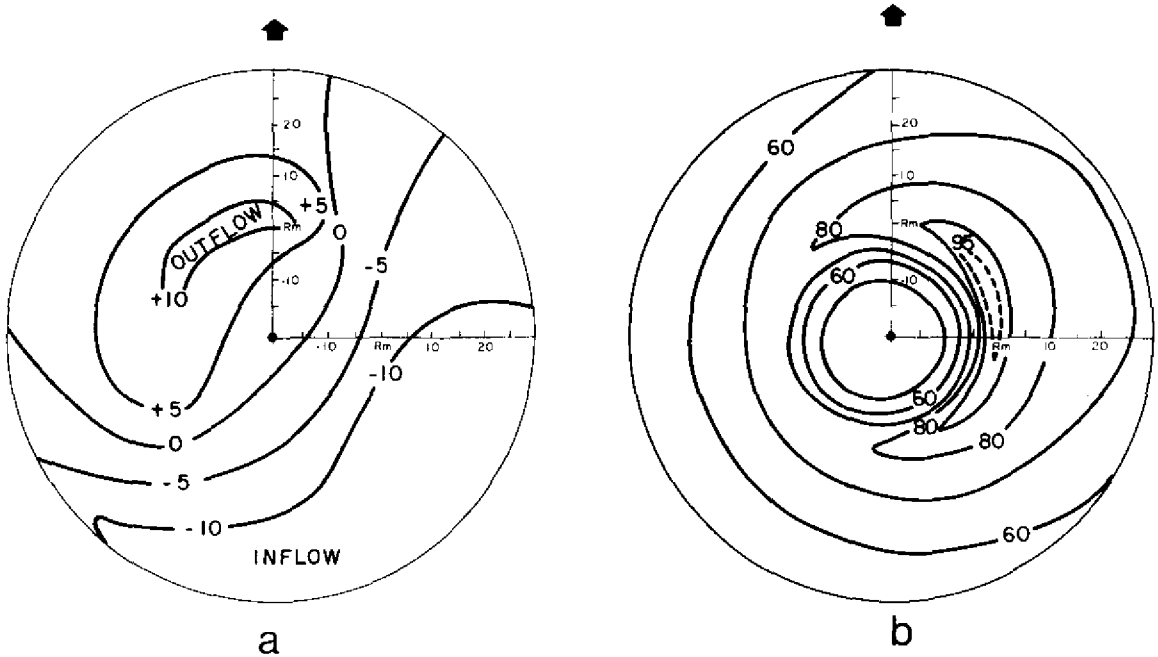

Figure 5. Mean radial (a) and tangential (b) winds at 1 km (900 millibars) in the inner core region of Atlantic hurricanes. The arrow indicates the direction of storm movement. Speeds are in kt., distance from the radius of maximum wind in n.mi. (After Shea and Gray 1973).

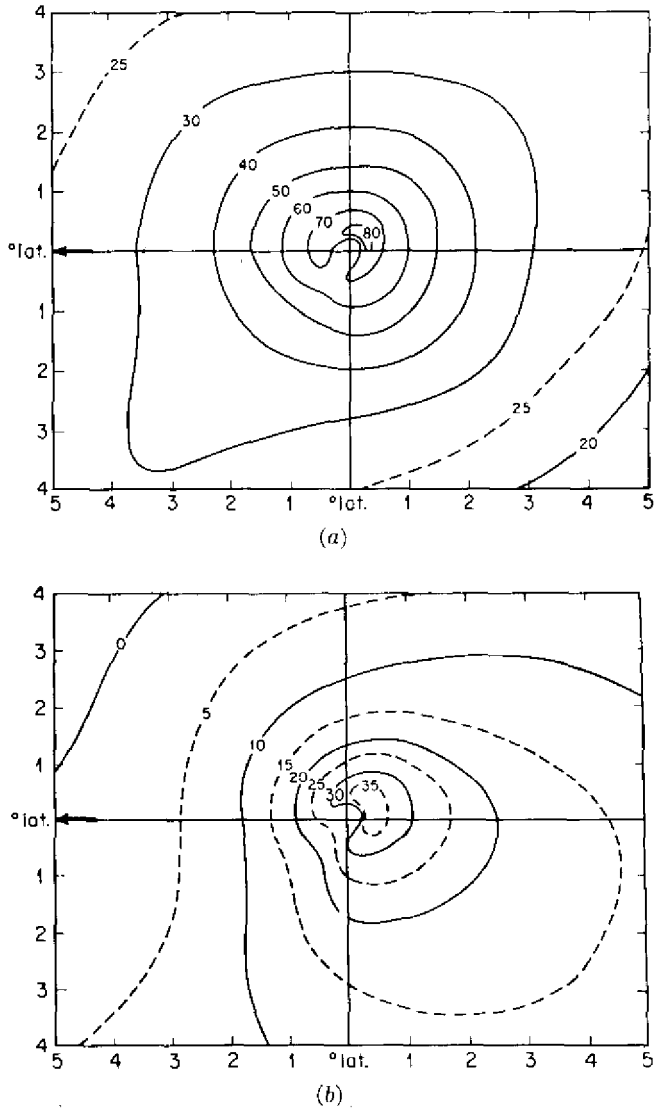

Figure 6. Mean tangential (a) and radial (b) winds, at about 300 m height, outside the inner core of Pacific typhoons. The arrow indicates the direction of storm movement. Speeds are in kt., distance in latitude degrees from the centre. (After Hughes 1952).

In constructing a best estimate of the wind field for the Bangladesh cyclone of 1970, the Shea and Gray patterns of Figure 5 were used as the basis of the wind field near the eye and the corresponding Hughes pattern provided guidance in extending the field out to greater distances. The centres of the patterns in Figure 5 were positioned 200 km from the radar site on a bearing of 196 degrees and were rotated to reflect the 23-degree heading of the storm at 0600Z of 12 November. Figures 7 and 8 show the estimated distributions of tangential and radial components in an area south of the radar site. The 95-kt contour of Figure 7 is in good agreement with the earlier observation that winds may have reached 100 kt.

4.0 Mapping the Doppler Wind Field

A Doppler radar detects only the component of wind velocity along the radar beam. Accordingly the wind components about the cyclone centre, portrayed in Figures 7 and 8, were used to compute wind components towards the radar site. The computations were made on a two-degree, 10-km grid over the area bounded by bearings of 180 and 210 degrees and ranges of 150 and 250 km. Over the balance of a field given by Figure 4b, a 10-degree and 50-km grid was used. At each grid point the tangential velocity, V_t and radial velocity, V_r were read from Figures 7 and 8 and the component of wind towards the radar, V_R was computed from the expression

$$V_R = V \cos (\beta - \theta)$$

where $V = (V^2_t + V^2_r)^{1/2}$,

θ is the bearing from the radar site in degrees,

R is the range from the radar site to km, and

β is the wind direction given by

$$\beta = 106 + \arctan \left\{ \frac{[R \sin (196-\theta)]}{[200-R \cos (196-\theta)]} \right\} + \arctan \frac{V_R}{V_T}.*$$

The data were then plotted at the grid points and contours (isotachs) were drawn, beginning at ± 3.7 kt, at the 7.42-kt interval that corresponds to the width of the colour bands of the radar display. Figure 9 shows the mapping of wind components towards the radar. The sign convention is that velocity away from the radar is positive.

Although the entire area contained in Figure 9 is unlikely to contain radar targets, it is instructive to code Figure 9 in colour according to

* When R > 200 km and θ > 196 degrees, the constant, 106 is replaced by 286.

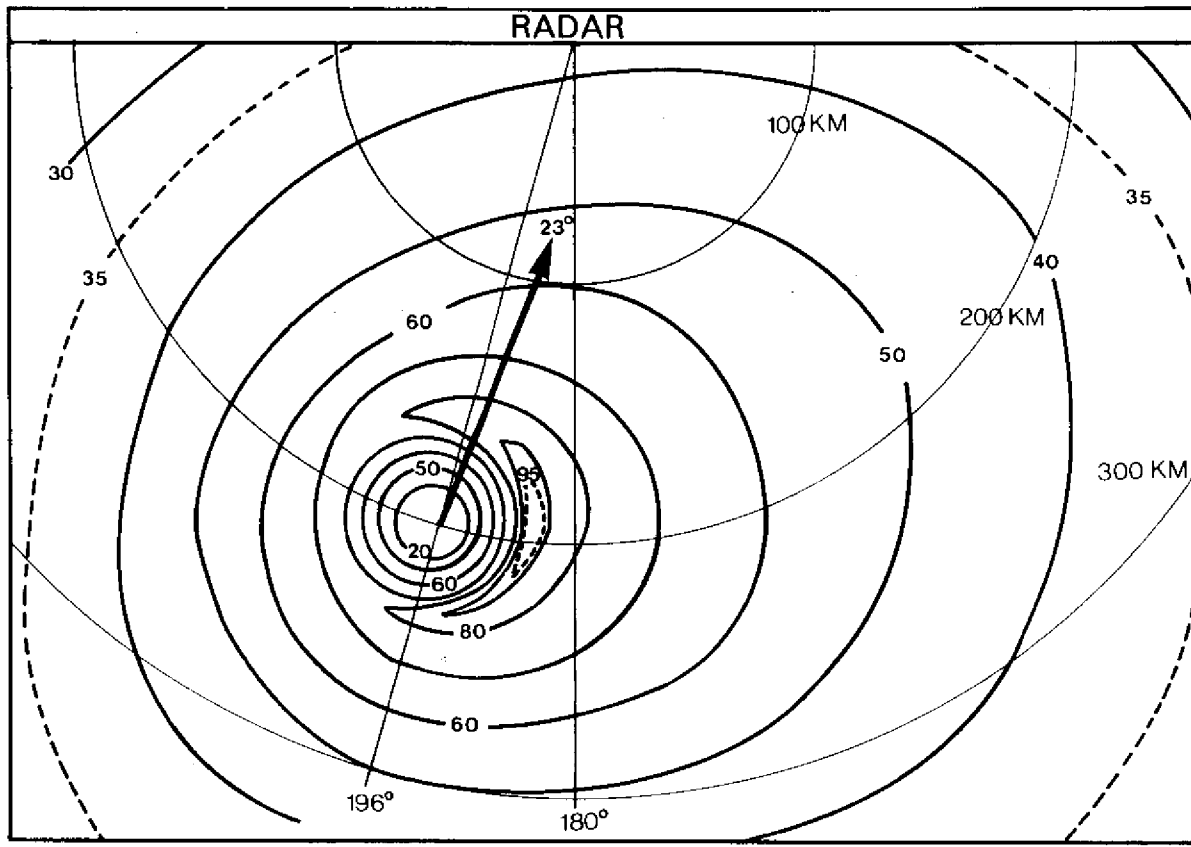

Figure 7. Estimated distribution of the tangential wind component around a tropical cyclone 200 km from the radar site, on a bearing of 196 degrees, moving on a heading of 23 degrees. Speeds are in kt.

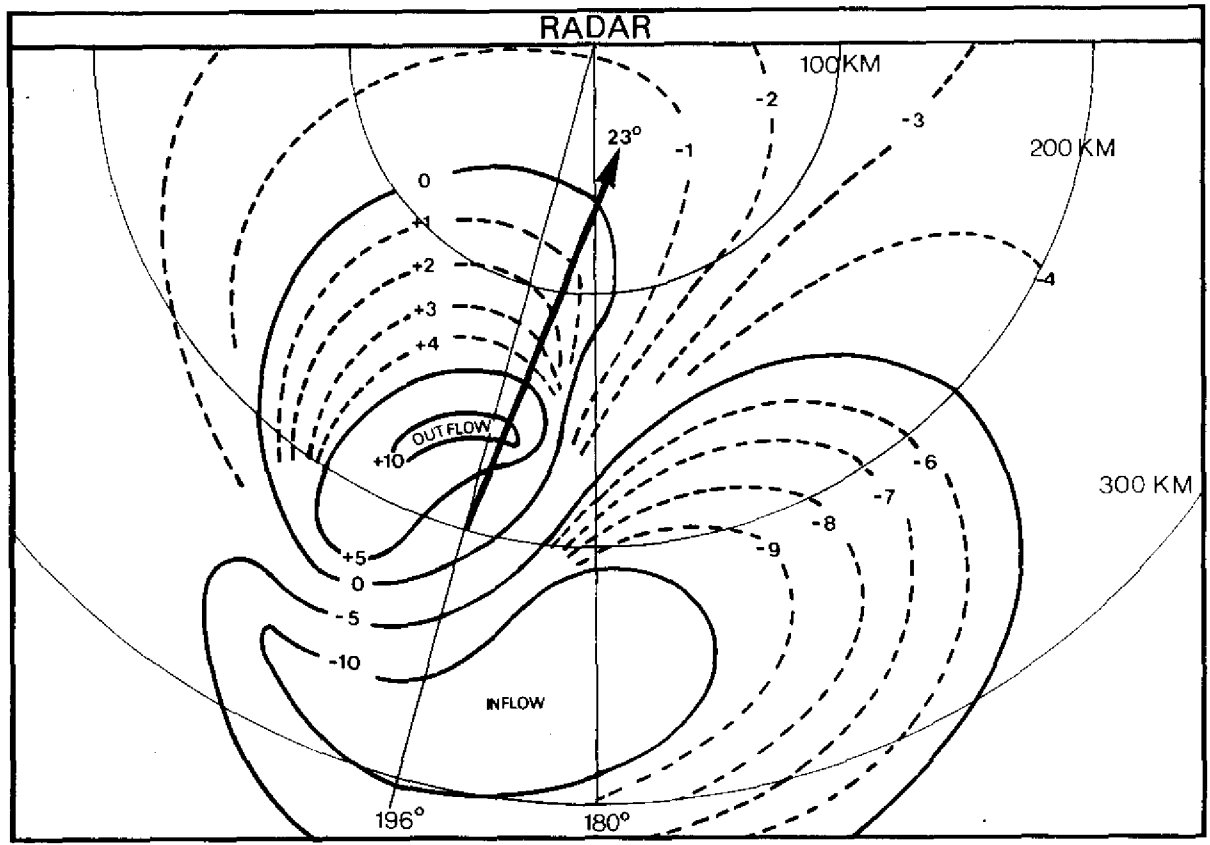

Figure 8. Estimated distribution of the radial wind component towards the centre of a tropical cyclone 200 km from the radar site, on a heading of 23 degrees. Speeds are in kt.

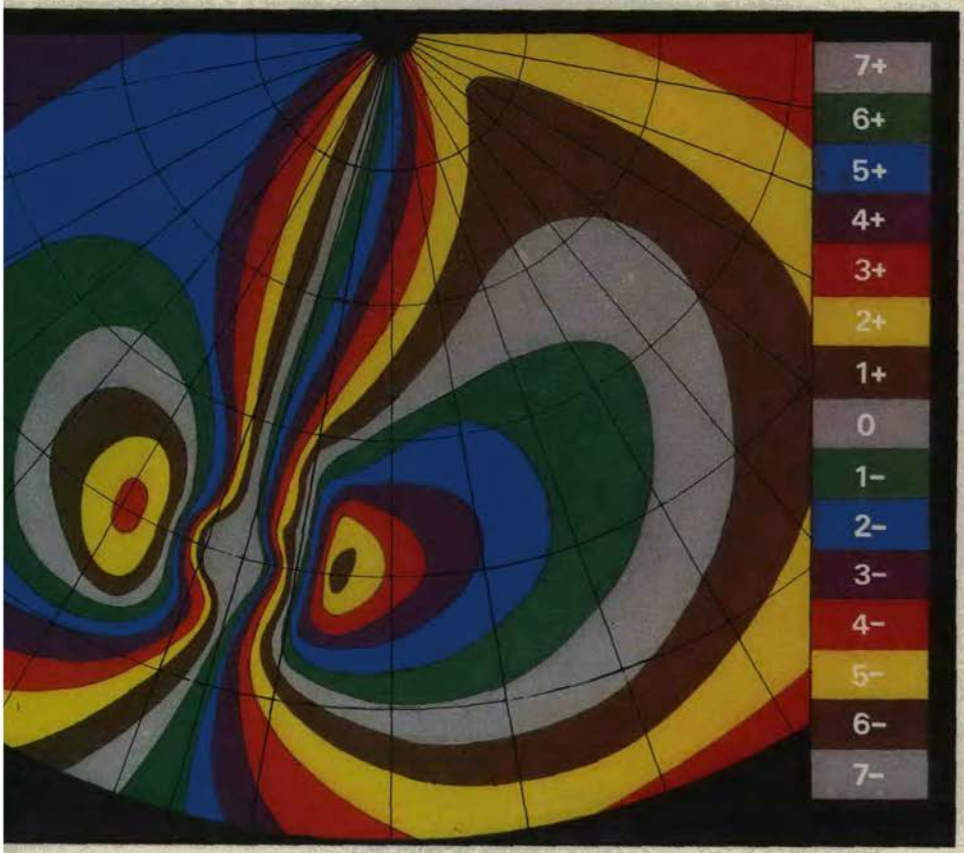

Figure 10. Distribution of the wind field of Figure 9 portrayed in colour according to the coding scheme of Figure 3.

the procedure suggested in Figure 3. The result of this portrayal is shown in Figure 10 along with a colour code bar for the range −55.7 to +55.7 kt. Examination of Figure 10 illustrates that colour ambiguities are not a problem. It is obvious that the shaft of grey radiating out from the radar site corresponds to the zero velocity band (−3.7 to +3.7) and the bulge in the shaft at a range of 200 km identifies the region of light winds at the eye of the cyclone. The other two appearances of the colour, grey, correspond to colour numbers −7 and +7 as shown on the colour code bar of Figure 10. Simply by counting, one can verify that the enclosed brown patch in the right half of the pattern is the thirteenth colour, corresponding to an average speed of 13 (7.42) = 96 kt. Similarly the oval red patch in the left half of the pattern is the tenth colour and corresponds to an average speed of 74 kt.

To provide an example of a non-killer storm, Figure 11 shows the colour coding of the wind pattern if wind speeds had been, everywhere, exactly one-half of those appearing in Figures 9 and 10. The brown patch in the right of Figure 11 is the sixth colour, average speed 6(7.42) = 45 kt; the blue patch in the left of the figure is the fifth colour, average speed 37 kt.

5.0 The Distribution of Radar Echoes

In general, less than the total patterns of Figures 10 and 11 will appear on a coloured display of radar echoes because radar targets will not completely fill the area. We cannot state exactly what the distribution of radar echoes might have been at 0600Z on 12 November 1970. For guidance we have the ample literature on hurricanes and cyclones as observed on radar (Wexler 1947; Dunn 1951; Byers 1954; Kessler and Atlas 1956; Colón *et al.* op cit.; Senn op cit.; Senn *et al.* 1972; Cantilo and Fernandez-Partagas 1972; Tang 1973). Certain general characteristics emerge. The radar echoes are arranged in bands spiralling in towards the "eye"; the "eye" is echo free. Regions largely free of echoes are found between the bands. The bands are narrowest near the "eye", broadening as they spiral out from the "eye". The number of bands varies from two to about eight.

It is somewhat harder to develop a consensus on the distribution of echoes in relation to the direction of motion of the cyclone. Echoes usually extend farthest from the eye in the forward right quadrant with minimum echoes in the two left quadrants; however, the humidity of the air being drawn in at the outer fringes of the cyclone can alter this. In reporting on a cyclone moving west south-westward near the

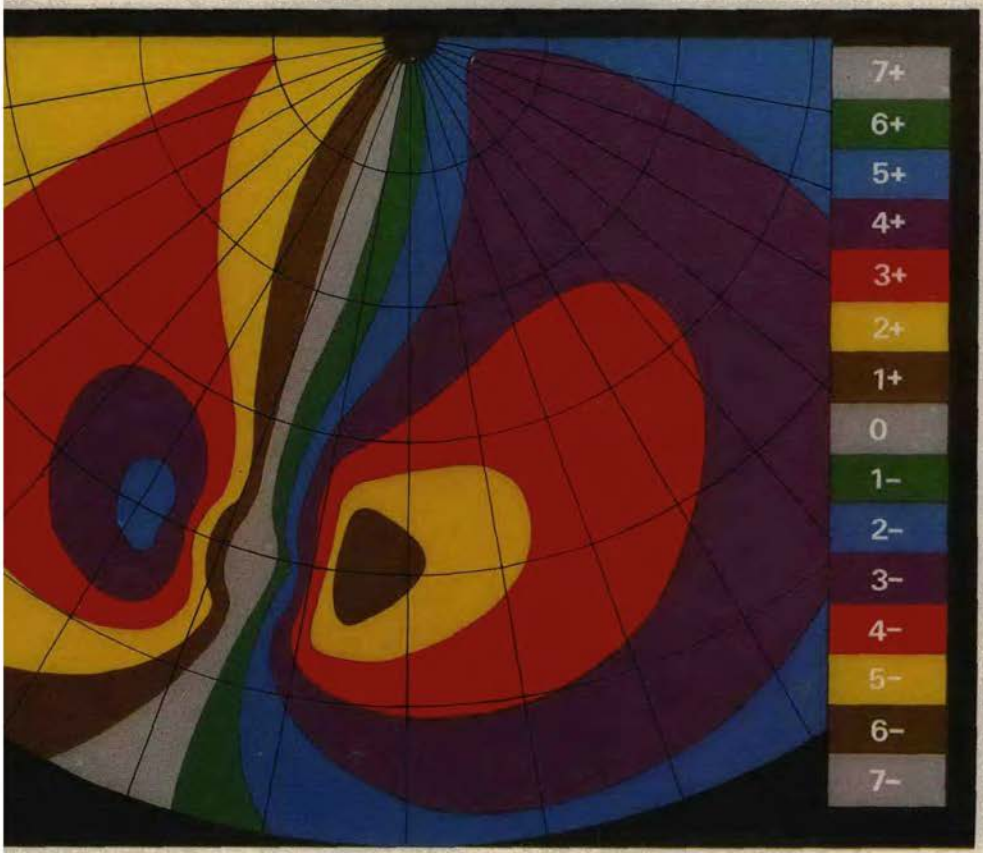

Figure 11. Colour portrayal of the component of wind towards the radar site for a tropical cyclone with half the intensity of the storm portrayed in Figure 10.

Figure 12. Estimated distribution of radar targets at 0600Z associated with the tropical cyclone of 12 November 1970. See text for basis of estimate.

coast of Arabia, Colón *et al.* (op. cit.) observed the heaviest echoes in the two left quadrants. In a radar study of precipitation associated with 20 typhoons, Tang (op. cit.) showed that heavy rain occurred in different quadrants depending upon the air masses that are in proximity to the typhoon. Since many of the available radar echoes of tropical cyclones are for northward moving Atlantic storms, the influx of drier air from North America may be partly responsible for the observed echo minimum in the left, rear quadrant.

As to the overall extent of the echo pattern, there are reports that the area of radar echoes is about an order of magnitude smaller than the area of the associated cloud cover seen in corresponding satellite pictures (Blackmer 1961; Fujita and Ushijima 1961; Kulshrestha and Gupta 1964; Kulshrestha 1970). As the last two references attest, the relationship applies to disturbances over the Bay of Bengal. Frank and Husain (op. cit) reported the cloud cover of the Bangladesh cyclone, as seen from ITOS 1, had a diameter of six to seven degrees of latitude (nearly 800 km). This would support a diameter of about 250 km for the radar echo.

Figure 12 represents the type of radar echo that probably was associated with the Bangladesh cyclone. Its characteristics are as follows:

(1) Echo-free eye with diameter 35 km
(2) Five spiral bands
(3) Greatest echo extent in the forward right quadrant
(4) Least echo extent in the rear left quadrant
(5) Total echo diameter about 250 km
(6) Greatest reflectivity in the eye wall cloud.

Undoubtedly the fine structure of Figure 12 would have been represented differently by another analyst. However, the fine structure tends to undergo constant change.

6.0 Portrayal of the Radar Echo in Colour

A console control permits one to display the radar echo in colour as shown in Figure 13. Figure 13 is obtained simply by overlaying Figure 12 on Figure 10. Clearly one may still confirm that wind speeds of about 96 kt are found to the right of the eye of the cyclone. If the storm had been a non-killer, the pattern would have been that shown in Figure 14 obtained by overlaying Figure 12 on Figure 11.

In practice it may happen that a gap between spiral bands is present in the region of maximum winds. The operator may then have to wait

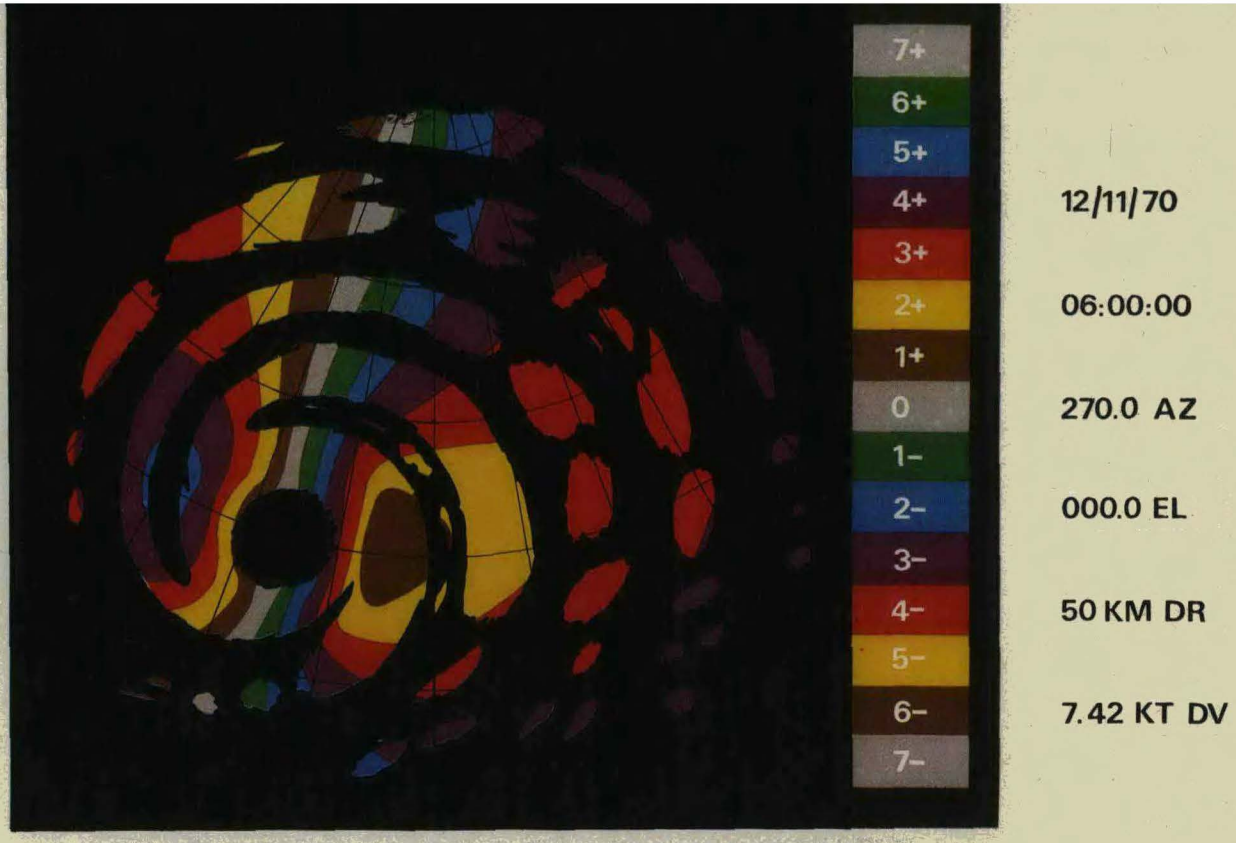

Figure 14. Portrayal of the radar pattern of Figure 12 with colour coding of Doppler velocities, for the non-killer cyclone of Figure 11. Legend on the right as it appears on radar display, reading from top to bottom: day/month/year; time in hours, minutes and seconds; antenna azimuth angle; antenna elevation angle; spacing of range marks; speed increment per colour band.

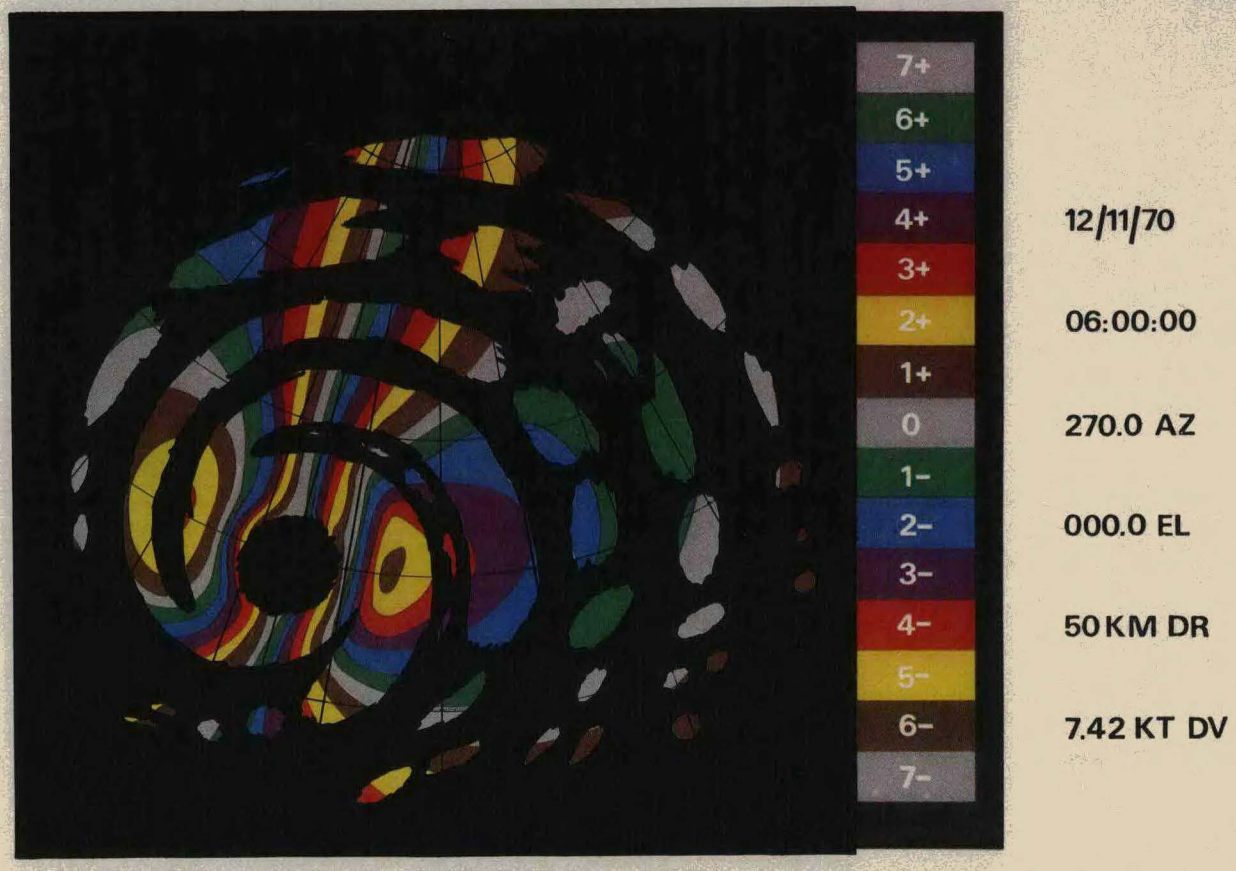

Figure 13. Portrayal of the radar pattern of Figure 12 with colour coding of Doppler velocities, for the killer cyclone of Figure 10. Legend on the right as it appears on radar display, reading from top to bottom: day/month/year; time in hours, minutes and seconds; antenna azimuth angle; antenna elevation angle; spacing of range marks; speed increment per colour band. (Note that

a few minutes until a rearrangement of the constantly changing banded structure provides the needed data. However, this is unlikely to be a problem since in the overwhelming majority of cases the maximum winds occur within the eye wall cloud (Shea and Gray 1973).

7.0 Discussion of the Errors and Limitations of the Procedure

The purpose of this section is to summarize the errors and limitations inherent in the use of Doppler radar with colour coding to detect cyclone severity. First, there must be radar echoes from the region of maximum wind. As pointed out above, maximum winds occur in the wall cloud. This almost guarantees strong echoes because of the ample moisture and substantial rain normally associated with the wall cloud. Dunn (1962) however cites one moderately severe Bay of Bengal tropical storm that had only a few sprinkles of rain under the wall cloud. To minimize this difficulty, we ensure that ample power is radiated by specifying a peak power of one million watts and by extending the pulse length. Although resolution decreases as pulse length increases, a pulse length of 4 μs would still provide an adequate 600 m of resolution. The minimum detectable reflectivity would then be 8 dBZ at a range of 200 km and 11 dBZ at a range of 300 km.* Here it is assumed that the beam is filled with falling precipitation particles. However, at 300 km range (recall that a one-degree beam would occupy the region 5.29 $\pm$2.62 km above msl) there will likely be times when this is not the case. The problem is unlikely to be serious for the more severe tropical cyclones, since they can be expected to have reflectivities well above 11 dBZ, in the lower part of the beam, to compensate for an absence of targets near the top of the beam. Further increases of either peak power or pulse length can provide still greater sensitivity if this is needed.

In the colour display of Figure 13 some colours are skipped because of the gaps in the echo, even though all colours appear in correct sequence in Figure 10. However, colour skips may also result from unusually large horizontal gradients. Generally, with a one-degree beam at a range of 200 km, colour skips begin to occur if the horizon-

* An antenna gain of 41 dB and a minimum signal detectable by the radar receiver of -108 dBm are assumed. Rather than attempt to define the difficult concept of reflectivity and the unusual unit, dBZ, some typical values are given. In drizzle the reflectivity can be as small as -10 dBZ. In rain in which each cubic metre of air contains 1000 drops, all 1 mm in diameter, the reflectivity is 30 dBZ. In hail, reflectivities as high as 70 dBZ are observed.

tal gradient exceeds 4.3 kt/km. Examination of horizontal gradients in the 533 radial legs presented by Gray and Shea (1976) showed that colour skips would be fairly common inside the radius of maximum wind, in extreme cases involving skips of up to four consecutive colours, but rare outside the radius of maximum wind. Even in the presence of such colour skips, careful reference to a standard colour bar covering the full range of possible speeds will ensure that speeds are correctly interpreted from colours.

The matter of data smoothing must also be considered. There is smoothing because each colour band covers a range of 7.42 kt. For example, the tenth colour identifies wind speeds of 74.2 ±3.7 kt. The smoothing effect is 3.7 kt if we always assign, to each colour band, its mean speed.

There is also smoothing because of the volume sampled by each pulse. The volume is a 600 m section of a one-degree cone. At a range of 200 km the average diameter of the sampled volume is 3.5 km (1.88 n.mi.). In preparing their summary of hurricane data collected by aircraft, Gray and Shea (1976) had information on wind speeds for every few hundred metres. They considered it advantageous to compute average values for 2.5-n.mi. (4.6-km) flight segments in order to smooth out small scale fluctuations. Since a certain amount of smoothing is evidently desirable, a one-degree beam with a 4 μs pulse length would not introduce too much smoothing. Eleven radial legs from the referenced Gray and Shea summary were tested to see how much smoothing a two-degree beam would produce. At a range of 200 km the peak wind was reduced an average of five to six per cent and one could project possible reductions of up to 12 per cent in extreme cases. Clearly a two-degree beam would introduce too much smoothing.

Another limitation of radar is the fact that the earliest information, gathered when the storm is still at a great distance, underestimates wind speeds in the boundary layer. To evaluate this effect a vertical profile of maximum tangential wind speed was constructed, based on Figure 10 of Shea and Gray (op. cit.). It showed that the maximum wind speed at a height of 2.35 km (the height of a zero-degree elevation beam at a range of 200 km) was six per cent less than the maximum at a height of 0.65 km. By the time the storm moves within 105 km the beam height is down to 0.65 km and the effect has disappeared.

It is interesting to note that aircraft reconnaissance estimates of

wind speed are also low. They are derived by a Doppler navigation system as the vector difference between the true airspeed and the aircraft motion relative to the ocean. Because the ocean moves under wind stress, the computed winds are too low by an amount calculated by Gray and Shea (1973) to be six to seven per cent.

Cyclone asymmetry, illustrated in Figure 5(b), also affects the estimates of storm severity. The winds to the right of the storm track are the strongest, being about 10 per cent stronger than directly in front of or behind the "eye". If the storm were viewed from the side instead of head on, the true maximum winds would be tangential to the radar. The most accurate estimates of cyclone severity are obtained when the angle between the storm track and a line through the radar and cyclone eye is very small. Since, unless the cyclone heads directly for the radar, this angle grows as the storm approaches, the best estimates of cyclone severity are obtained when the cyclone is still a considerable distance from the radar.

8.0 The Related Problem of Predicting Storm Surges

In an operational warning system for tropical cyclones, the final step is the prediction of the accompanying storm surge. Given accurate data on the intensity of the cyclone and its track, reasonably accurate forecasts of the storm surge are possible.

Generally, storm surge is computed as some function of shoreline characteristics, angle of crossing the coast and the cyclone characteristics. Different procedures make use of different cyclone characteristics chosen from among central pressure, wind speed, radius of maximum wind, translational speed of the storm, total storm radius and so forth. Since the hydrostatic rise in sea level is only about 1 cm for each millibar drop in pressure, the contribution of low pressure to the total storm surge is measured in tens of centimetres or generally no more than 15 per cent of the total surge. Clearly wind contributes a good deal more than pressure to the surge. Unless both central pressure and maximum wind speed are known, one is often estimated from the other. But the relationship between the two variables is subject to wide variation as shown by Shea and Gray (op. cit.). For example, maximum wind speeds based on central pressure are subject to underestimates of as much as 40 kt and central pressures based on wind speeds are subject to overestimates of as much as 25 mb. Therefore, since wind speed makes a larger direct contribution than pressure to the total storm surge, if estimates are needed, it is preferable

to estimate central pressure from a measured speed than to estimate speed from a measured pressure. It should be noted that the Doppler radar provides direct and continuous measures of wind speed and radius of maximum wind, and the forward progress of the cyclone centre can be followed on the display.

Following the disastrous storm of 1970, Das (1972) made some preliminary computations of the magnitude of the storm surge near Chittagong, where the maximum storm surge was believed to have been 1.5 m. He had access to the Frank and Husain data (op. cit.) on storm track and severity and used a model storm with a radius of maximum wind of 30 km, a maximum wind speed of 100 kt, a central pressure of 960 mb, a 50 mb fall from the outer periphery to the centre and 20 km/hr as the translational speed of the storm. Although his computed value, 3.2 m, exceeded the reported surge at Chittagong, according to Frank and Husain, even larger surges occurred about 100 km to the west on the island of Bhola. More recently, Das *et al.* (1974) confirmed these preliminary computations and extended them by considering what the surge would have been if the same storm had struck the coast at two other points.

Flierl and Robinson (1972) also addressed the problem of "deadly surges in the Bay of Bengal". They drew attention to the significance of the right angle the coastline makes just north of Chittagong, pointing out that, for such a configuration, the surge includes both a direct contribution and a contribution reflected from the neighbouring coastline. As a result, the maximum response is almost double that of the same storm approaching a straight coastline. Their model storm was the same as the one used by Das (op. cit.) with the added specification of an 80 mi. storm radius.

They summarized their computations for the northern Bay of Bengal in a generalized graphical method for estimating storm surge. The predictors are the point of landfall, the storm heading (measured clockwise from a line through Chittagong and Cox's Bazar), the maximum wind speed and the translational speed of the storm. Storm surges were obtained by this method for eight severe storms that struck the area from 1960-70. The estimates were reasonably close to the reported values although, according to Frank and Husain, accurate reporting of storm surges in this area date from 1968 when an excellent network of tide gauges was installed along the coast.

Simpson (1974) has summarized investigations into storm surge prediction. He explains why surges occur only when the depth of

water becomes less than 90 m and gives an account of results obtained in the United States with NOAA's SPLASH Model for storm surge prediction. In January 1977, the World Meteorological Organization announced the imminent publication of *Manual on Storm Surge Prediction* by Miyazaki, Das and Jelesnianski.

9.0 Conclusions

Modern Doppler radars equipped with minicomputers for real time processing of velocity data and with colour displays of the processed data have been used successfully to portray wind fields of extratropical cyclones and hail supercells. In the present analysis, a set of specifications is developed for a cyclone detection radar suitable for use over the northern tip of the Bay of Bengal. The specifications are summarized below in Table 2. A rigid radome over the antenna would also be required to permit continued operation during high winds.

Table 2 Specifications of cyclone detection radar

Type	Coherent Doppler
Wavelength	10.7 cm
Transmitted power	One million watts peak
Pulse repetition frequency	500 per second
Pulse duration	Four microseconds
Beam width and pattern	One degree circular
Antenna	Circular, 7.7 metre diameter
Receiver sensitivity	Able to detect signal of −108 dBm
Maximum unambiguous range	300 km
Maximum unambiguous velocity	13.38 metre/second (26.0 kt).

Data on the average structure of tropical cyclones were used to estimate the wind field associated with the killer storm of 12 November 1970. When the wind field was portrayed in colour in the manner that it would appear on the colour display, an unambiguous signature of 96 kt winds was provided. It was further shown that the radar system was able to distinguish between killer and non-killer storms.

Credible warnings of tropical cyclones over Bangladesh are possible only if one can determine wind speeds accurately before the storm crosses the coast. In their report of eight Bangladesh cyclones, Flierl and Robinson (op. cit.) gave translational speeds ranging between 10 and 21 kt. For storms travelling at these speeds, assuming that the storm is detected at a range of 300 km, the radar system described in

the present analysis could provide warning from seven to 16 hours before the storm crosses the coast.

The cost of such a radar with radome would be $1-$2 million, while a suitable, heavy, weather-reconnaissance aircraft with adequate range would cost $4-$8 million. The radar can be operated at a cost of about $100,000-$150,000 per year including two full-time people for operations and maintenance. The aircraft can be operated, for 200 to 300 hr/yr, at a cost of $400,000-$600,000, including one flight crew, fuel and depreciation. If more hours are flown the cost of fuel and maintenance will increase. Radar costs are thus seen to be about a quarter of aircraft costs, both for initial acquisition and operation.

10.0 Acknowledgements

I have relied heavily on an unpublished set of notes by Dr. P. L. Smith, South Dakota School of Mines and Technology, Rapid City, South Dakota, as a general reference on radar meteorology. In addition to offering encouragement, Dr. R. J. Serafin, NCAR, Boulder, Colorado, read each draft of the work and provided many helpful suggestions that have been incorporated into the text. Professor R. A. Houze, Jr., University of Washington, Seattle, also read the manuscript and provided helpful suggestions. Mr. D. Shea, NCAR, generously supplied me with recent reports on cyclone structure that are not in the open literature. I am also grateful to Dr. K. A. Browning, Meteorological Office Research Unit, Royal Signals and Radar Establishment, Malvern, whose penetrating comments led to a number of revisions and served also as a reminder that the methodology I have advocated can only be verified by field trials with actual tropical cyclones. I want to express my appreciation to Ms. C. Lewsey and Mr. R. Wilkinson of Chelsea College, London, for their co-operation and professional skills in the preparation of and photography of the illustrations. Finally, I am greatly indebted to Dr. R. E. Munn, Atmospheric Environment Service, Toronto, who made it possible for me to visit MARC.

APPENDIX 1

A Simple Expression for Ray Tracing

Microwave radiation leaving the earth at an elevation angle less than 90 degrees is bent downward. Since its downward curvature is less than the curvature of the earth, even when the elevation angle is zero, the ray rises to higher elevations. Under average refractive conditions the position of the ray relative to the earth can be represented by a straight line ray and an earth surface with radius of curvature, $a = 4/3\ r$, where r is the radius of the earth (Freehafer 1951). Since the average value of r is 6371 km, a is approximately 8500 km.

We wish to know the height above mean sea level (msl) of a target at known slant range and elevation angle. Referring to the sketch, the radar is located at O and the target at P. The notation is as follows:

- Z – height of the target above msl
- R – slant range of the target
- α – elevation angle of the target
- Z_0 – height of the radar above msl
- z' – the portion of Z caused by earth curvature and refraction.

From the figure we can write

$$Z = z' + Z_0/\cos\beta + R \sin\alpha/\cos\beta \qquad (1)$$

Now $\beta < R/a$ radians, therefore $\cos\beta > \cos R/a$. Also, because $R \ll a$, $\cos\beta \approx 1$. The approximation is reasonably good out to R = 1200 km where $\cos R/a = 0.9900$, and excellent at R = 500 km where $\cos R/a = 0.9983$. Accordingly equation (1) can be written with acceptable accuracy as

$$Z = z' + Z_0 + R \sin\alpha \qquad (2)$$

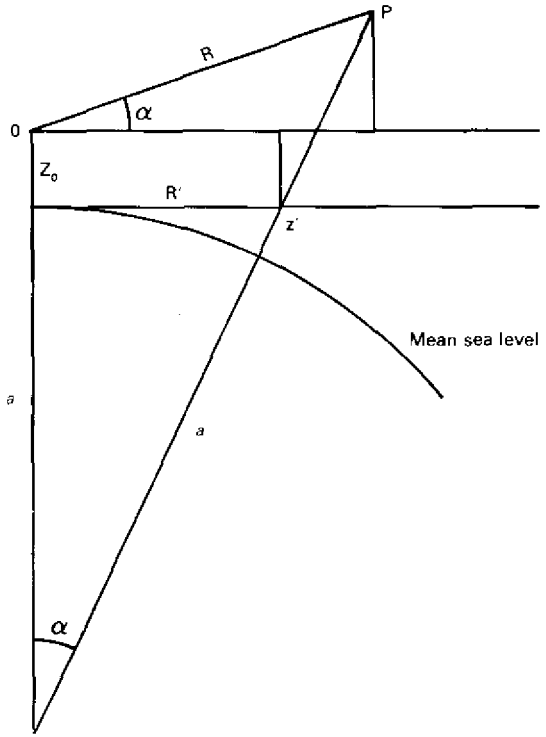

To obtain an expression for z', referring to the figure we have

$$R'^2 + a^2 = (z' + a)^2, \text{ or}$$
$$R'^2 = 2az' + z'^2. \tag{3}$$

An exact solution for z' is

$$z' = -a + (a^2 + R'^2)^{1/2}$$

but since $z'^2 \ll 2az'$ in (3) we may write

$$z' \approx R'^2/2a. \tag{4}$$

From the sketch we see that

$$R' = R\cos\alpha - R\sin\alpha\tan\beta - Z_0\tan\beta \tag{5}$$

This exact expression for R' can be used to evaluate z', but it is computationally awkward. We consider three approximations to R' as follows.

First approximation	:	$R' = R\cos\alpha - R\sin\alpha\tan\beta$
Second approximation	:	$R' = R\cos\alpha$
Third approximation	:	$R' = R$ (6)

In the first approximation we have dropped the last term in (5). If the radar is at sea level this term is zero and in any case it is always small because β and hence $\tan\beta$ are small. In the second approximation we have dropped the second term in (5) as well. It, too, tends to be small because it contains the product of two small terms, since α is also small in practice when viewing distant targets in the troposphere and lower stratosphere. The third approximation would be poor at large values of α but at large α, the only targets of interest are at such short range that z' is unimportant in equation (2) compared to $R \sin\alpha$.

Values of R' computed from the exact expression and the three approximate expressions are given in Table A-1 for selected values of R, α and Z_0. The associated values of z' and Z were computed from equations (4) and (2). Values of Z are given in Table A-2. The values of R and α were selected so that $Z<20$ km since targets of interest will be no higher than 20 km. The largest range used in Tables A-1 and A-2, 750 km, is the maximum unambiguous range when the pulse repetition frequency is a low 200/sec.

Table A-1

Values of R', computed from an exact expression and three approximate expressions, for selected values of R, α and Z_0. Distances in km, $\tan\beta$ set equal to R/8500.

R	50	200	300	750
α, in degrees	22.4	0.5	0.0	−1.2
Z_0	0.0	1.5	0.0	2.0
R' exact	46.115	199.916	300	751.048
R' approx. 1	46.115	199.951	300	751.225
R' approx. 2	46.227	199.992	300	749.836
R' approx. 3	50.000	200.000	300	750.000

Table A-2

Values of Z based on the values of R′ given in Table A-1. Distance in km.

R	50	200	300	750
α, in degrees	22.4	0.5	0.0	−1.2
Z_0	0.0	1.5	0.0	2.0
Z exact	19.179	5.596	5.294	19.474
Z approx. 1	19.179	5.597	5.294	19.490
Z approx. 2	19.179	5.598	5.294	19.367
Z approx. 3	19.201	5.598	5.294	19.381

Computations of R′ and Z were made for four other cases. For the eight cases, the error in Z introduced by using the third approximation were 22, 2, 0, 93, 25, 7, 33 and 19 m. Clearly the third approximation, equation (6), is sufficiently accurate. Accordingly we may write

$$z' = R^2/2a = R^2/17{,}000$$

and finally, as our simple working expression,

$$Z = R^2/17{,}000 + R \sin\alpha - Z_0.$$

Footnote: This expression for ray tracing has been in use for a number of years, especially by graduates of the Department of Atmospheric Science at Massachusetts Institute of Technology. However, after spending considerable time trying to find the source of the expression, the writer has found it necessary to derive it again.

Reference:

Freehafer, J. E. (1951), "Geometrical optics", *in Propagation of Short Radio Waves*, Kerr, D. E., ed., Mass. Inst. Tech. Radiation Lab. Ser., No. 13, 53. McGraw-Hill.

11.0 References

Baynton, H. W., Frush, C. L., Serafin, R. J., Hobbs, P. V., Houze, R. A., Jr. and Locatelli, J. D. (1977), "Real-time wind measurements in extratropical cyclones using Doppler radar", accepted for publication in J. Appl. Met.

Blackmer, R. H., Jr. (1961) "Satellite observations of squall line thunderstorms", *Proc. 9th Weather Radar Conf.*, 76-82, Amer. Met. Soc., Boston.

Browning, K. A. and Foote, G. B. (1976), "Airflow and hail growth in supercell storms and some implications for hail suppression", *Quart. J. R. Met. Soc.*, **102**, 499-533.

Byers, H. R. (1954), "The atmosphere up to 30 kilometres". In *The earth as a planet*, Kuiper, G. P., ed., 344-357. Univ. Chic. Press., Chicago.

Cantilo, L. M. H. and Fernandez-Partagas, J. J. (1972), "Analysis of a tropical depression based on radar data", *J. Appl. Met.*, **11**, 298-303.

Colón, J. A., Raman, C. R. V. and Srinivasan, V. (1970), "On some aspects of the tropical cyclone of 20-29 May 1963 over the Arabian Sea", *Indian J. Met. Geoph.*, **21**, 1-22.

Das, P. K. (1972), "Prediction model for storm surges in the Bay of Bengal", *Nature*, **239**, 211-213.

Das, P. K., Sinha, M. C. and Balasubramanyam, V. (1974), "Storm surges in the Bay of Bengal", *Quart. J. R. Met. Soc.*, **100**, 437-449.

Dunn, G. E. (1951), "Tropical cyclones". In *Compendium of Meterology*, 887-901. Amer. Met. Soc., Boston.

Dunn, G. E. (1962), "The tropical cyclone problem in East Pakistan", *Mon. Wea. Rev.*, **90**, 83-86.

Dvorak, V. F. (1972), US National Oceanic and Atmospheric Administration, Nat. Env. Sat. Serv. Tech. Memo (NOAA TM NESS 36) 15 pp.

Flierl, G. R. and Robinson, A. R. (1972), "Deadly surges in the Bay of Bengal: dynamics and storm-tide tables", *Nature*, **239**, 213-215.

Frank, N. L. and Husain, S. A. (1971), "Deadliest tropical cyclone in history?", *Bull. Amer. Met. Soc.*, **52**, 438-444.

Freehafer, J. E. (1951), "Geometrical optics", in *Propagation of Short Radio Waves*, Kerr, D. E., ed., Mass. Inst. Tech. Radiation Lab. Ser., **No. 13**, 53. McGraw-Hill.

Fujita, T. and Ushijima, T. (1961), "Investigation of squall lines with the use of radar and satellite photographs", *Proc. 9th Wea. Radar Conf.*, 186-192, Amer. Met. Soc., Boston.

Gray, G. R., Serafin, R. J., Atlas, D., Rinehart, R. E. and Boyajian, J. J. (1975), "Real-time color Doppler radar display", *Bull. Amer. Met. Soc.*, **56**, 580-588.

Gray, W. M. and Shea, D. J. (1973), "The hurricane's inner core region. II. Thermal stability and dynamic characteristics", *J. Atmos. Sci.*, **30**, 1565-1576.

Gray, W. M. and Shea, D. J. (1976), "Data summary of NOAA's hurricane inner-core radial leg flight penetrations 1957-1967 and 1969", Atmos. Sci. Paper no. 257, Dept. of Atmos. Sci., Colo. State Univ., 243 pp.

Hughes, L. A. (1952), "On the low level wind structure of tropical cyclones", *J. Met.* **9,** 422-428.

Jordan, E. S. (1952), "An observational study of the upper wind-circulation around tropical storms", J. Met. **9,** 340-346.

Kessler, E., III and Atlas, D. (1956), "Radar synoptic analysis of hurricane Edna, 1954". USAF CRC Geophysical Research Papers, **No. 50,** 113 pp.

Koteswaram, P. (1971), "A decade of satellite meteorology in India", *Indian J. Met. Geoph.*, **22,** 273-278.

Kulshrestha, S. M. (1970), "Spiral bands in monsoon depressions over northern India", *Preprint Vol. 14th Radar Met. Conf.* 367-368, Amer. Met. Soc., Boston.

Kulshrestha, S. M. and Gupta, M. G. (1964), "Satellite study of an inland monsoon depression", *Indian J. Met. Geoph.*, **15,** 175-182.

Lhermitte, R. M. (1972), "Real time processing of meteorological Doppler radar signals", *Preprint Volume: 15th Radar Meteorology Conference*, 364-367. Amer. Met. Soc., Boston.

Senn, H. V. (1971), "Radar hurricane research, Sept. 1, 1970-Aug. 31, 1971". Miami (Florida) Univ. Rosenstiel School of Marine and Atmospheric Sciences, ML 71095, 37 pp. and appendices.

Senn, H. V., Andrews, G. F. and Courtright, C. L. (1972), "Radar hurricane research, Sept. 1971 to 31 Dec. 1972". Miami Univ. Rosenstiel School of Marine and Atmospheric Sciences, Contract No. N22-67-72(N), final report to NOAA, Dec. 1972. 30 pp.

Shea, D. J. and Gray, W. M. (1973), "The hurricane's inner core region. I. Symmetric and asymmetric structure", *J. Atmos. Sci.*, **30,** 1544-1564.

Sikka, D. R. (1971), "Evaluation of the use of satellite photography in determining the location and intensity changes of tropical cyclones in the Arabian Sea and the Bay of Bengal", *Indian J. Met. Geoph.*, **22,** 305-312.

Simpson, R. H. (1974), "The complex killer", *Oceanus*, **17,** 22-27. Woods Hole, Massachusetts.

Tang, C. H. (1973), "Radar study of typhoon precipitation patterns and their relations to floods", Proc. India-Philippines Symposium on Tropical Cyclones and Tropical Meteorology, Quezon City, 1972, 68-75. WMO/UNDP Project Meteorological Training and Research, Manila, Tech. series No. 23.

Wexler, H. (1947), "Structure of hurricanes as determined by radar", *Ann. N.Y. Acad. Sci.*, **48,** pp. 821-844.